

Article

# Uncertainty Handling in Structural Damage Detection via Non-Probabilistic Meta-Models and Interval Mathematics, a Data-Analytics Approach

Ramin Ghiasi <sup>1</sup>, Mohammad Noori <sup>2,\*</sup>, Wael A. Altabey <sup>1,3</sup>, Ahmed Silik <sup>1</sup>, Tianyu Wang <sup>1</sup> and Zhishen Wu <sup>1</sup>

<sup>1</sup> International Institute for Urban Systems Engineering (IIUSE), Southeast University, Nanjing 210096, China; rghiasi.s@gmail.com (R.G.); wael.altabey@gmail.com (W.A.A.); silikth@gmail.com (A.S.); ty\_wang@seu.edu.cn (T.W.); zsw@seu.edu.cn (Z.W.)

<sup>2</sup> Department of Mechanical Engineering, California Polytechnic State University, San Luis Obispo, CA 93405, USA

<sup>3</sup> Department of Mechanical Engineering, Faculty of Engineering, Alexandria University, Alexandria 21544, Egypt

\* Correspondence: mnoori@outlook.com; Tel.: +1-805-903-2411

**Featured Application:** The proposed novel approach, presented in this paper, can effectively interpret complex sensor data collected for structural health monitoring and offers a reliable scheme for damage detection of structural systems.

**Abstract:** Recent advancements in sensor technology have resulted in the collection of massive amounts of measured data from the structures that are being monitored. However, these data include inherent measurement errors that often cause the assessment of quantitative damage to be ill-conditioned. Attempts to incorporate a probabilistic method into a model have provided promising solutions to this problem by considering the uncertainties as random variables, mostly modeled with Gaussian probability distribution. However, the success of probabilistic methods is limited due the lack of adequate information required to obtain an unbiased probabilistic distribution of uncertainties. Moreover, the probabilistic surrogate models involve complicated and expensive computations, especially when generating output data. In this study, a non-probabilistic surrogate model based on wavelet weighted least squares support vector machine (WWLS-SVM) is proposed to address the problem of uncertainty in vibration-based damage detection. The input data for WWLS-SVM consists of selected wavelet packet decomposition (WPD) features of the structural response signals, and the output is the Young's modulus of structural elements. This method calculates the changes in the lower and upper boundaries of Young's modulus based on an interval analysis method. Considering the uncertainties in the input parameters, the surrogate model is used to predict this interval-bound output. The proposed approach is applied to detect simulated damage in the four-story benchmark structure of the IASC-ASCE SHM group. The results show that the performance of the proposed method is superior to that of the direct finite element model in the uncertainty-based damage detection of structures and requires less computational effort.

**Keywords:** surrogate models; uncertainties; non-probabilistic; interval analysis; wavelet packet decomposition (WPD); data analytics



**Citation:** Ghiasi, R.; Noori, M.; Altabey, W.A.; Silik, A.; Wang, T.; Wu, Z. Uncertainty Handling in Structural Damage Detection via Non-Probabilistic Meta-Models and Interval Mathematics, a Data-Analytics Approach. *Appl. Sci.* **2021**, *11*, 770. <https://doi.org/10.3390/app11020770>

Received: 17 December 2020

Accepted: 9 January 2021

Published: 15 January 2021

**Publisher's Note:** MDPI stays neutral with regard to jurisdictional claims in published maps and institutional affiliations.



**Copyright:** © 2021 by the authors. Licensee MDPI, Basel, Switzerland. This article is an open access article distributed under the terms and conditions of the Creative Commons Attribution (CC BY) license (<https://creativecommons.org/licenses/by/4.0/>).

## 1. Introduction

In general, civil structures are prone to damage during their service life, leading to the loss of their serviceability and safety. Thus, the integrity and the state of the health of these structural systems is essential for structural safety assessment and decision-making management [1]. Although significant progress has been made in this area, the high level of variability due to noise and other interferences, the uncertainties associated with data collection, structural performance, and in-service operational environments pose

significant challenges in finding the necessary information to support decision-making [2,3]. In addition to the effect of measuring noise, some uncertainties are due to undamaged stiffness in real structures, which is also caused by reasons such as connections, infills, and others [4]. Normally, the natural frequencies of the structure are used as damage-sensitive feature because of ability to estimate the condition of the structure even if a small number of sensors are installed [3,5]. However, estimation based on natural frequencies is sensitive to environmental and operational variables (EOVs), and in practice the structural acceleration response is usually used [4].

Moreover, despite advancements in computer capacity, the enormous computational cost of running complex engineering simulations makes it impractical to rely solely on simulation for structural health monitoring applications [6]. To cut down the cost, surrogate models, also known as meta-models, are constructed and then used in place of the actual simulation models [7]. The effectiveness of surrogate models when applied in vibration-based damage detection has been demonstrated in numerous studies [7,8]. However, in the face of uncertainty, the use of surrogate models has been questioned in terms of their reliability [9].

Surrogate models in damage detection suffer from two inevitable uncertainties: modeling error and measurement noise [10]. The existence of error in finite element (FE) modeling, due to the inaccuracy of physical parameters and non-ideal boundary conditions, and also finite element discretization, together with nonlinear structural properties, may result in generating the vibration parameters from such an FE model not exactly representing the relationship between the modal parameters and the damage parameters of the real structure [11]. On the other hand, the presence of a measurement error in the collected data, which is usually used in a surrogate model as the test data, is often inevitable. Since the efficacy of the prediction of a surrogate model relies on both components' accuracy, the existence of these uncertainties may result in false and inaccurate predictions. Thus, it is necessary to analyze the effect of uncertainties on surrogate model's reliability for structural damage detection.

Ghiasi et al. [12] and Bakhary et al. [13] demonstrated the effect of uncertainties on the output of support vector machine (SVM) and artificial neural networks (ANNs) in training and testing results, and proposed the use of a probabilistic surrogate model that considered the presence of uncertainties in the FE model and the measurement data. Their research work showed that the probabilistic approach can facilitate accurate detection of damage even in noisy data [12,13]. However, the probabilistic methods presented in the literature suffer from several shortcomings, such as assuming uncertain parameters as random variable with a Gaussian distribution with a given variance that subsequently produce statistical structural damage results [13]. In practice, the probability density function cannot be accurately obtained because of the complexity of uncertainty sources [14]. Moreover, the assumption of Gaussian distribution for uncertain parameters is not valid. In addition, the lack of experimental data reduces the possibility to obtain a suitable probability density function. Creating an acceptable and reliable probabilistic model also requires different data sets in order to train and upgrade the model. This data set is created through finite element analysis or simulation by utilizing surrogate models such as ANN algorithms or response surface method [13]. This approach requires an iterative simulation procedure that takes a very long time and, again, mostly relies on the Gaussian assumption.

Due to these challenges and shortcomings, Qiu and Wang [15] emphasized the need to introduce non-probabilistic interval analysis methods. Unlike the standard probabilistic approach, no assumptions about uncertainty distributions for estimating the probability of damage existence (PoDE) are needed for the non-probabilistic interval approach. Only the upper and lower bounds of uncertain variables are needed, thereby simplifying the detection of damage with noisy data and reducing complex computation compared to the probabilistic approach [9,16].

In this paper, the applicability of non-probabilistic methods is extended by using a non-probabilistic surrogate model based on wavelet weighted least squares support vector

machine (WWLS-SVM) [17,18]. This surrogate model is a combination of weighted least squares support vector machine (WLS-SVM) [19] and thin plate spline Littlewood–Paley wavelet kernel function, which is called WWLS-SVM [17]. The input data for this model consists of extracted features of acceleration response of structures, and the output is the Young's modulus (E values), which acts as an elemental stiffness parameter (ESP). Through the interval analysis method [9,10], noise in the measured response of the structure is considered to be coupled rather than statistically distributed.

The interval bound (lower and upper bounds) of the ESP changes is computed based on an interval analysis method. By considering the uncertainties in the input parameters, the surrogate models are used to predict this interval-bound output. A possibility of damage existence (PoDE) parameter is used for the undamaged and damaged states to determine the relationship between the input and output parameters [20]. To provide an indicator of damage severity, the damage measure index (DMI) suggested by Wang et al. [21] is adopted.

The proposed method's feature extraction phase will be carried out using wavelet packet decomposition (WPD) method [22]. In this study, the measured structural dynamic response is decomposed into wavelet component functions [23]. Then wavelet packet relative energies of these components are used as input of the proposed meta-model.

The proposed method's applicability is demonstrated by performing damage detection on the 4-story building of Phase I of IASC-ASCE SHM benchmark [24]. The results show that the proposed method is able to accurately determine the location and the severity of damage in structural elements by considering the uncertainties caused by modeling and noise in the sensors.

The main contributions of this paper may be summarized as follows:

1. In this study, a non-probabilistic wavelet packet transform method is proposed that resolves the problem of uncertainties in vibration-based damage detection. The damaged and undamaged structure's acceleration responses are decomposed to obtain the wavelet packet relative energies of the signal.
2. Different levels of detection of structural damage, including the occurrence of damage, location and severity of it, are evaluated using a computational approach. Furthermore, the effect of different levels of uncertainties on damage identification are presented.
3. Furthermore, the applicability of WWLS-SVM to act as a non-probabilistic surrogate model for damage detection of structures, with consideration of uncertainties, will be examined through simulating a damage in the benchmark model.

This paper is organized as follows. In Section 2, three main steps of the proposed method are defined. Feature extraction method utilizing wavelet packet transform (WPT) is described in Section 3. The procedure of using interval analysis method for the consideration of uncertainties in the proposed scheme is presented in Section 4. In Section 5, a description of WWLS-SVM is given. Evaluation of the proposed method on structural health monitoring (SHM) benchmark is studied in Section 6, and Conclusions are presented in Section 7.

## 2. Main Steps of the Proposed Damage Detection Procedure

The main focus of this research is to facilitate the assessment of uncertainties in SHM. Accordingly, an integrated system, consisting of three steps, will be proposed in this paper. Firstly, wavelet packet decomposition (WPD) [17,23] is applied to the structural acceleration response under ambient vibration, and feature vectors are obtained by a feature extraction based on wavelet energy spectrum. Subsequently, interval analysis method is used to incorporate uncertainties in the model using the upper and lower bounds of extracted features. In the final step, by considering the uncertainties in the input parameters, the WWLS-SVM is used to predict the output of this interval bound.

Figure 1 summarizes the proposed novel method based on WPD, interval analysis, and WWLS-SVM, which consists of three main steps, as stated before. Each step will be explained in more detail in the following section.

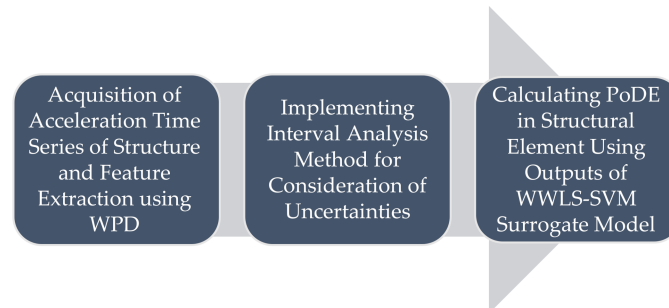


**Figure 1.** Summary of non-probabilistic damage detection approach.

### 3. Feature Extraction Using Wavelet Packet Transform (WPT)

Non-stationary signals are frequently encountered in a variety of engineering fields (e.g., wind, ocean, and earthquake engineering) [25]. The inability of conventional Fourier analysis to preserve the time dependence and describe the evolutionary spectral characteristics of non-stationary processes requires tools which allow time and frequency localization beyond customary Fourier analysis. The wavelet transform is used to decompose random processes into localized orthogonal basis functions, providing a convenient format for the modeling, analysis, and simulation of non-stationary processes [26]. The time and frequency analysis made possible by the wavelet transform provides insight into the character of transient signals through time-frequency maps of the time variant spectral decomposition that traditional approaches miss [25].

Wavelet packet component energy is an effective method to define and characterize a specific signal phenomenon in the time-frequency domain. Yen and Lin's [27] demonstrated that the energy stored in a specific frequency band, at a certain level of wavelet packet decomposition, provides more potential for signal feature than the coefficients alone. Sun and Chang [28] utilized sensitivity analysis, to compare the four damage indices of frequency, modal, flexibility, and energy changes of wavelet packets. They subsequently concluded that the index based on wavelet packet energy had the best performance in detecting changes in elemental stiffness. Therefore, in this study, this method will be used for the feature extraction phase of the proposed method.

The WPT of a time domain signal  $f(t)$  can be calculated using a recursive filter-decimation operation [29]. After  $j$ -levels of decomposition, the original signal  $f(t)$  can be expressed as:

$$f(t) = \sum_{i=1}^{2^j} f_j^i(t), \quad (1)$$

$$f_j^i(t) = \sum_{k=1}^{2^j} C_{j,k}^i(t) \psi_{j,k}^i(t), \quad (2)$$

Herein, a linear combination of wavelet functions  $\psi_{j,k}^i(t)$  can express the component signal  $f_j^i(t)$ . Integers  $i, j$  and  $k$  are the parameters of the modulation, scale and translation, respectively;  $C_{j,k}^i(t)$  and  $\psi_{j,k}^i(t)$  are defined as the wavelet packet coefficients and the wavelet packet function. The wavelet packet coefficients can be obtained from.

$$C_{j,k}^i = \int_{-\infty}^{\infty} f(t) \psi_{j,k}^i(t) dt, \quad (3)$$

Frequency domain information is very important in damage detection of structures. Therefore, a high level of WPT is required to detect small changes in the signal. After

WPT is carried out, the corresponding energies of these decomposed component signals can be used to assess the condition of the structure. The component energies of signal are expressed as follows:

$$E_j^i = \int_{-\infty}^{\infty} f_j^i(t)^2 dt, \quad (4)$$

It can be proven that, when the mother wavelet is semi-orthogonal or orthogonal [30], the signal energy  $E_f$  is the summation of the  $j$ -level component energies as follows:

$$E_f = \int_{-\infty}^{\infty} f^2(t) dt = \sum_{i=1}^{2^j} E_j^i, \quad (5)$$

In this research, the relative energy corresponding to the component signals of the structural acceleration response has been used as WWLS-SVM input, thus, the relative energy  $E_i$  in  $i$ -frequency band can be expressed as:

$$E_i = \frac{E_j^i}{E_f}, \quad (6)$$

Battle–Lemarie is a symmetric wavelet basis function. In the frequency domain, this wavelet feature is a band filter, while the scale function is a lowpass filter. Consequently, the above two functions' frequency bands are overlapped in certain degree, indicating a desirable orthogonal feature [31]. Orthogonal wavelets represent the signal with as little information as possible, and without redundancy. These features are very useful in denoising and in matrix multiplications [32]. So Battle–Lemarie is adopted as the basis wavelet package function in this paper to decompose the signals to be analyzed into different frequency bands and make each frequency band energy independent and irredundant [33]. Several optional measuring nodes are chosen, and vibration signals from these nodes are analyzed by using the WPT.

Apart from the effect of selecting the mother wavelet function, the decomposition level of analysis, at which the wavelet analysis should be performed, has immense effect on the performance of wavelet-based methods. Reasonable level requirements are not known in advance and depend on a broad range of parameters, including structural characteristics, signal characteristics and type, location and severity of the damage, etc. Different decomposition levels have been suggested by several researchers [34].

In this paper based on our previous work [17,35] The level of decomposition of the wavelet packet is determined using both healthy and damaged structural models and set on 7 levels [17]. The frequency band energy is then calculated and normalized. The wavelet package relative energy of the signals from sensor  $s$  is:

$$E_p^s = \{E_m, m = 1, \dots, M\}, \quad (7)$$

where,  $s = 1, 2, \dots, S$ ,  $p$  is the acquiring number,  $p = 1, 2, 3, \dots, P$ .

The wavelet package relative energy (WPRE)  $E_p^s$  of the signals from sensor  $s$  is combined to obtain the fused feature vector [17]:

$$E_p = \{E_p^1, E_p^2, \dots, E_p^s\}. \quad (8)$$

This fused feature vector will be used as the input of the surrogate model after implementing interval analysis method.

#### 4. Interval Analysis Method for Consideration of Uncertainties

The interval bounds can provide supports for structural health monitoring under uncertain conditions [36]. The general concept of interval mathematics is implemented by supplying the upper and lower boundaries of input parameters to generate the upper and

lower boundaries of output parameters to consider the two uncertainties (epistemic and aleatory uncertainty). Artificial intelligence based surrogate models, such as the WWLS-SVM scheme, usually establish the relationship between the input and output via a black box procedure [37], therefore, the fundamental equation of interval analysis proposed by Polyak and Nazin [36] can be directly applied to the input parameters (extracted features) to produce the intervals of the output parameters (ESP values). It is noteworthy to indicate that, in black box-based methods, the algorithm’s accuracy is checked by evaluating the output responses of the algorithm and comparing them with the training data.

As shown in Equation (9), the stiffness reduction ratio (SRF) indicates the changes in the stiffness parameter for each member of the structure:

$$SRF = 1 - \frac{\alpha_d}{\alpha_u}, \tag{9}$$

where:

$\alpha_d$  = value of ESP in the damaged state

$\alpha_u$  = value of ESP in undamaged (healthy) state.

The intervals of the ESPs and extracted features for both states can be formulated as follows [9]:

$$[\underline{\alpha}] \approx [E_p] = \text{lower bound of ESP value}, \tag{10}$$

$$[\bar{\alpha}] \approx [\bar{E}_p] = \text{upper bound of ESP value}, \tag{11}$$

The upper and lower bounds of  $\alpha$  and  $E_p$  are denoted by the upper and lower bars, respectively. Therefore, the interval bounds for each parameter can be obtained as:

$$E_p = [E_p, \bar{E}_p] = \{E_p^1, E_p^2, \dots, E_p^s\}, E_p^s = [E_p^s, \bar{E}_p^s], \tag{12}$$

$$\alpha_c^I = [\underline{\alpha}_c^I, \bar{\alpha}_c^I] = \{\alpha_{c1}^I, \alpha_{c2}^I, \dots, \alpha_{ck}^I\}^T, \alpha_{ck}^I = [\underline{\alpha}_{ck}^I, \bar{\alpha}_{ck}^I], \tag{13}$$

where:

$c$  = number of damage cases.

$k$  = number of segments of structures.

$I$  = interval number or vector representation

$s$  = number of sensor on structure

$p$  = is the acquiring number

And the input and output middle values are indicated as:

$$x^c = m(x) = \frac{(\underline{x} + \bar{x})}{2}, \tag{14}$$

In the above equation, the variable  $x$  represents the exact values of the extracted features (input values) and the output of the algorithm (ESPs). The upper and lower bars show the upper and lower bounds of  $x$ , respectively. Thus, the training and testing functions of the WWLS-SVM are established based on Equations (10)–(14). The uncertainties are coupled with extracted features in terms of the interval bounds. These features are used as input parameters of the surrogate model, while the ESPs ( $\alpha$ ) are used as outputs. Finally, two WWLS-SVM models, which include the lower bound and upper bound analyses, are provided, as shown in Table 1.

**Table 1.** Input and output variables for training and testing of WWLS-SVM.

	Surrogate Model	Training Input	Testing Input	Output
Lower bound	WWLS-SVM 1	$\frac{E_p^{Ir}}{p} = E_p^{Ir}$ of Acc. response with negative $\omega$	$\frac{E_p^{Ie}}{p} = E_p^{Ie}$ of Acc. response with negative $\omega$	$\underline{\alpha}_{ck}$
Upper bound	WWLS-SVM 2	$\frac{E_p^{Ir}}{p} = E_p^{Ir}$ of Acc. response with positive $\omega$	$\frac{E_p^{Ie}}{p} = E_p^{Ie}$ of Acc. response with positive $\omega$	$\overline{\alpha}_{ck}$

The variable  $\omega$  indicates the uncertainty level in the acceleration signal. The interval variables of training and testing data are presented herein using superscripts *Ir* and *Ie*. The lower and the upper bounds of the input parameters are applied through the + and – values of the uncertainties in two surrogate models of WWLS-SVM 1 and WWLS-SVM 2.  $\underline{\alpha}_{ck}$  and  $\overline{\alpha}_{ck}$  are the outputs of the WWLS-SVM models and show the boundaries of the predicted ESPs of damage case c. Once the lower and upper boundaries of the ESPs are obtained, the possibility of damage existence (PoDE) are subsequently calculated and then the damage severity is measured using damage measure index (DMI). Definition of these indexes will be explained in the next section.

As shown in Table 1, it is noteworthy to indicate that only two WWLS-SVM models are needed to predict the lower and the lower bounds of ESP, which is less than the conventional method presented in previous articles. In fact, in proposed methods for probabilistic damage detection of structures, several surrogate models are usually used. In the method presented by Bakhary et al. [13], Which is based on the point estimate method [38], 4 neural network models are utilized and in the method presented by Ghiasi et al. [12], which is based on a Monte Carlo simulation algorithm, 200 least squares support vector machine (LS-SVM) models are used. Employing fewer surrogate models reduces the overall prediction error. In probabilistic methods, increasing the prediction error results in an increase in the standard deviation of the probability distribution function, which in turn reduces the accuracy of the probability of damage existence (PDE).

*Possibility of Damage Existence (PoDE) and Damage Measure Index (DMI)*

The PoDE is calculated by comparing the ESPs vectors in both healthy and damaged modes. As shown in Table 1, the vectors are the lower and upper boundaries of ESPs, which are also the output of WWLS-SVM models (refer to Table 1), respectively. The terms are as follows:

$$\alpha_u^I = \{ \alpha_{u1}^I, \alpha_{u2}^I, \dots, \alpha_{uk}^I \}^T, \tag{15}$$

$$\alpha_d^I = \{ \alpha_{d1}^I, \alpha_{d2}^I, \dots, \alpha_{dk}^I \}^T, \tag{16}$$

where  $\alpha_u^I$  shows the interval bound for the undamaged ESP ( $[\overline{\alpha}_{uk}, \underline{\alpha}_{uk}]$ ) and  $\alpha_d^I$  shows the interval bound for the damaged ( $[\overline{\alpha}_{dk}, \underline{\alpha}_{dk}]$ )

Figure 2 illustrates the intersection of the intervals of the damaged and undamaged ESPs on the same axis, where the shaded region indicates the PoDE. The middle value ( $x^c$ ) disparity between the two states will increase as the damage increases. The PoDE ranges from 0 to 100%, with 100% indicating a relatively high possibility of damage to that particular element and 0% indicating no damage.

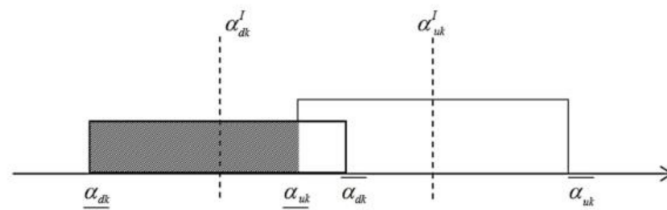


Figure 2. Scheme for PoDE.

The areas of damage and undamaged ESP on two separate axes are shown in Figure 3. The possible damage area is shown by a single solid rectangle where the failure plane for both states is equal. The shaded region reflects the ESP damage. Compared to the undamaged ESP, since the ESP damage is greater, the PoDE is defined as the ratio of the area of damage region to the total area of the entire region. The quantitative measurement of the PoDE can therefore be described as below [9]:

$$PoDE = \frac{A_{damage}}{A_{total}} \times 100\%, \tag{17}$$

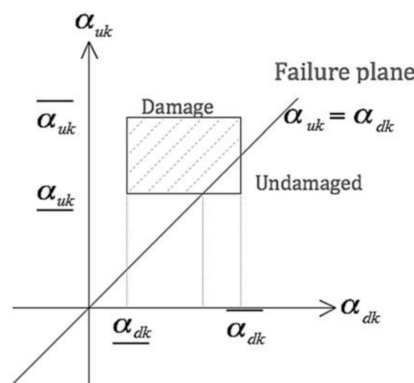


Figure 3. Space for damage and undamaged ESP.

The interval value of damaged and undamaged ESP will have significant variations in reality, as the PoDE would be 100%. Therefore, using PoDE alone will not provide an accurate or direct indication of the damage. Accordingly, the damage measure index (DMI) is calculated as below [9]:

$$DMI = SRF \times PoDE. \tag{18}$$

### 5. Wavelet Weighted Least Squares Support Vector Machine (WWLS-SVM)

In this study, WWLS-SVM is used as the main surrogate model for addressing the problem of uncertainty in vibration damage detection. Fundamentally, support vector machine (SVM) is a machine learning method based on statistical learning theory (SLT), introduced by Cortes and Vapnik [39]. The LS-SVM is an extended version of standard SVM [40]. In the LS-SVM, a sum-squared error (SSE) cost function has been substituted by Vapnik’s  $\epsilon$ -insensitive loss function. In addition, instead of inequalities, the LS-SVM considers equality type constraints as in the classic SVM method [40]. This reformulation simplifies the problem significantly by directly solving a series of linear equations rather than a convex quadratic program (QP).

In this paper, the weighted version of LS-SVM [41] will be used as a surrogate model. WLS-SVM was introduced as a highly effective machine learning algorithm in large-scale problems by Suykens et al. [41]. In fact, the assignment of weights to both the SVM and the least square version of SVM (LS-SVM) results in a more robust and accurate function prediction [42].

Wavelets as kernel functions have been introduced and developed in ANNs and SVMs [43,44]. Wavelet kernel functions have been demonstrated to be superior to other kernel functions in ANN and SVM training. [44]. Accordingly, the kernel function of WLS-SVM is substituted with a specific type of wavelet function proposed by Ghiasi et al. [17]. In fact, the thin plate spline Littlewood–Paley wavelet is used as the kernel function of WLS-SVM. Finally, this WLS-SVM based on wavelet kernel function is called WWLS-SVM. For further detailed information on the mathematical basis of WWLS-SVM algorithm, readers are referred to the original work by the main authors [15], and the work reported in [39].

## 6. Damage Detection of IASC-ASCE Structural Health Monitoring Benchmarks

The structure shown in Figure 4 is a 4-storey building with a base plan of 2.5 by 2.5 m and a total height of 3.6 m. This structure is a model with a quarter scale model of a physical structure which was developed in the Earthquake Engineering Research Laboratory of the University of British Columbia (UBC) [24] for benchmark studies. The material characteristics of this model are as follows: hot rolled grade 300 W,  $F_y = 300$  MPa (42.6 kpsi).

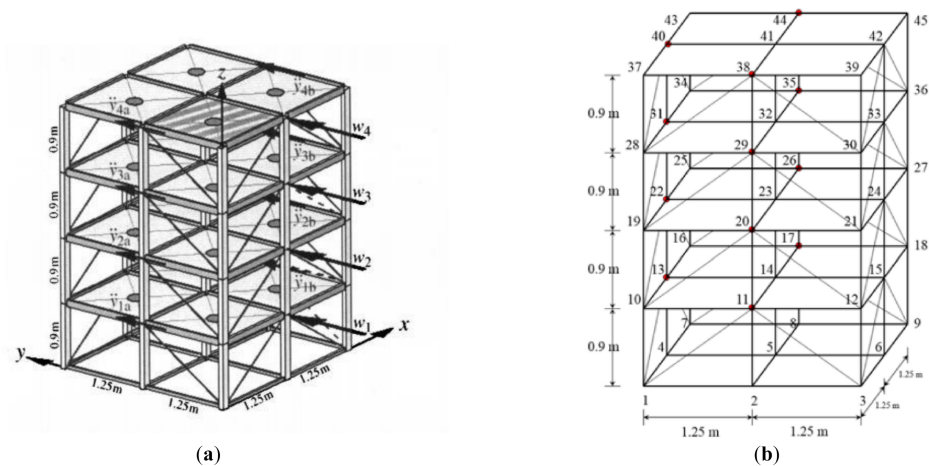


**Figure 4.** ASCE benchmark structure used for health monitoring: (a) The analytical model [24] (b) Distribution of node numbering.

The primary aim of the IASC-ASCE benchmarks is to provide a common platform for researchers in the field of structural health monitoring to apply different SHM methods to an identical structure and to compare their results [45]. The benchmarks comprise of two phases, e.g., Phase I and Phase II, each with simulated and experimental data. In this study, for prediction of structural damage, Phase I simulated data generated from this structure are employed. The excitation is low-level ambient wind loading at each floor in  $y$ -direction. To consider the uncertainty of environmental loads, the wind loading is modeled as filtered Gaussian white noise process passed through a sixth-order low-pass Butterworth filter with a 100 Hz cutoff [17]. The sensors are placed on each floor on the middle column of each face of the structure. Therefore, a total of 16 sensors are installed on the structure. The input signal used in this paper is the acceleration response recorded by the sensor installed on column 4. The location of these sensors is shown in Figure 5, which includes nodes 13, 22, 31, and 40. The sampling frequency is 100 Hz and the length of each recorded response is 40,000. As stated in Azimi and Pekcan work [46] measured acceleration response data acquired by conventional Micromachined Microelectromechanical Systems (MEMS) sensors.

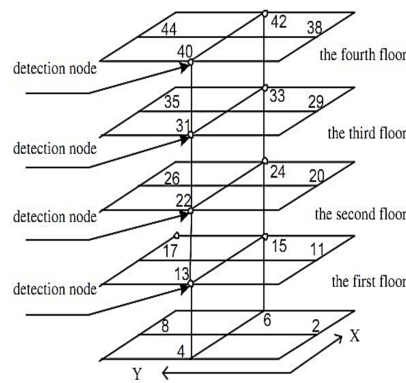


Figure 5. Location of all structure’s sensors and the sensors used in this research.

The two types of Finite Element (FE) models with 12 and 120 degrees of freedom (DOF), respectively, are used to produce the time histories for pre-defined damage cases and damage patterns described in Table 2 [24]. Acceleration response of damage scenarios in Table 2 is used to test the performance of the proposed model.

Table 2. Damage Cases of the Benchmark Model [45].

Description	Case				
	1	2	3	4	5
12 DOF model					
120 DOF model	○	○	○	○	○
Symmetric Mass	○	○	○	○	○
Asymmetric Mass				○	○
Ambient Excitation	○	○		○	○
Shaker on Roof			○	○	○
Damage Patterns: Remove Followings					
(1) All Braces in the 1st Story		○	○	○	○
(2) All Braces in the 1st and 3rd Story	○	○	○	○	○
(3) One Brace in the 1st Story	○	○	○	○	○
(4) One Brace in the 1st and 3rd Story				○	○
(5) 4 and Loosen Floor Beam at 1st Level				○	○
(6) 2/3 Stiffness in One Brace at 1st Story					○

It is worth noting that, the MATLAB® code (MATLAB® R2015b-Mathworks) for the structural model was obtained from the network for earthquake engineering simulation (NEES) Database for Structural Control and Monitoring Benchmark Problems [47]. We use this source code (with predefined damage scenario of phase I) without any modification for validation of proposed algorithm. This phase deals with analysis considering shear building model. Therefore, the discrepancies, i.e., user-defined damage, between analytical model and real model were not considered. In Phase II, the freedom for user to define the type and point of damage has been included [48].

6.1. Feature Extraction and Training Phase for Damage Cases 4 and 5

Since the damage cases 4 and 5 are more inclusive and are also more complex damage scenarios, they will be used to assess the merits of the proposed algorithm. Training data is generated by simulating damage cases 4 and 5 on a three-dimensional structure with 12-DOF. Damage is induced by reducing the stiffness parameter of each story. The mathematical expression of which is as follows:

$$k_{ij}^{pd} = \theta_{ij} k_{ij}^u \tag{19}$$

where  $\theta_{ij}$  is the stiffness loss parameters for the  $i^{\text{th}}$  story ( $i = 1, \dots, 4$ ) and face  $j$  ( $j = +x, -x, +y, -y$ ) (see Figure 6). Furthermore,  $k_{ij}^u$  are stiffnesses of the undamaged shear building model, e.g.,  $k_{i,+x}^u = k_{i,-x}^u = 34.0 \text{ MN/m}$  and  $k_{i,+y}^u = k_{i,-y}^u = 53.5 \text{ MN/m}$  [45]. The damage severities are expressed as stiffness reduction factor (SRF)  $\theta_{ij}$ .

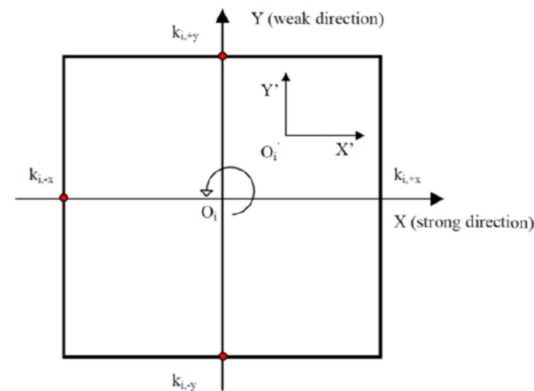


Figure 6. Floor Plan for Benchmark Structure.

After imposing damage, recorded acceleration response of the structure from each of 4 sensors (Figure 5) are decomposed using the procedure described in Section 3. The Battle–Lemarie [32] wavelet is used as a basic function to analyze the output acceleration response of the sensors. According to the WPE process, up to 7 levels of decomposition are conducted. Based on this approach, 128 frequency bands with a width of 3.91 Hz will be created. The resulting energy components are arranged according to their magnitudes 95% of the WPRE is mostly distributed below 100 Hz frequency bands, which are both important in value and sensitive to the damage occurred in the structure. Therefore, WPT's first 8 component energies are selected as damage features.

Extracted features from different sensors are fused to construct input vectors of the surrogate model as expressed in Equation (8). Training output vectors for the first and second surrogate model are damage severities which is expressed in Equation (19) as stiffness reduction factor  $\theta_{ij}$ . In the first phase, to construct the damage signatures for the purpose of comparing the performance of PoDE and PDE [13], 50% stiffness reduction is imposed on the stiffness in the X and Y directions (single damage level). When the damage is assigned, the stiffness of both elements facing each other, e.g., elements in +Y and −Y faces, are reduced together. In the second phase, to evaluate the damage severity index (DMI), two levels of damage, i.e., 30 and 70% of stiffness losses, are imposed on the structural elements in order to create the training dataset.

### 6.2. First Phase—Comparing the Performance of PoDE and PDE

In order to validate the proposed method, a comparison between PoDE and PDE indices is performed, as shown in Table 3. PDE values have been calculated based on the probabilistic surrogate method presented by Ghiasi et al. [49]. The acceleration response of full benchmark models with 12 and 120 DOF is used for damage cases 4 and 5. To consider the measurement noise, the acceleration responses of the structure are contaminated with Gaussian white noise (WGN). For the noise levels considered, the signal-to-noise ratios (SNRs) is: (i) 5%, SNR 26 dB. The SNR is expressed as:

$$SNR = 20 \log_{10} \left( \frac{1}{n} \right). \quad (20)$$

where  $n$  is the noise level.

**Table 3.** PoDEs and PDEs for Damage Cases 4–5.

Damage Case	Damage Patten	Story 1		Story 2		Story 3		Story 4	
		$\theta_{i,y}$	$\theta_{i,x}$	$\theta_{i,y}$	$\theta_{i,x}$	$\theta_{i,y}$	$\theta_{i,x}$	$\theta_{i,y}$	$\theta_{i,x}$
Target Damage Cases 4&5	1	100	100	0.00	0.00	0.00	0.00	0.00	0.00
	2	100	100	0.00	0.00	100	100	0.00	0.00
	3	0.00	100	0.00	0.00	0.00	0.00	0.00	0.00
	4	0.00	100	0.00	0.00	100	0.00	0.00	0.00
	5	0.00	100	0.00	0.00	100	0.00	0.00	0.00
	6	0.00	100	0.00	0.00	0.00	0.00	0.00	0.00
Prediction Damage Case 4 PoDE	1	100	100	0.00	0.00	0.00	0.00	0.00	0.00
	2	100	100	0.00	0.00	100	100	0.00	0.00
	3	2.00	100	0.00	0.00	0.00	0.00	0.00	0.00
	4	0.00	100	0.00	0.00	100	0.00	0.00	0.00
Prediction Damage Case 5 PoDE	1	100	98	0.00	0.00	0.00	0.00	0.00	0.00
	2	98	100	2.00	4.00	100	95	0.00	0.00
	3	2.00	97	0.00	0.00	0.00	0.00	0.00	0.00
	4	4.00	100	0.00	0.00	100	1.00	0.00	0.00
	5	0.00	100	0.00	0.00	100	0.00	0.00	0.00
	6	0.00	99	0.00	0.00	0.00	0.00	0.00	0.00
Prediction Damage Case 4 PDE	1	100	99	0.00	0.00	0.00	0.00	0.00	0.00
	2	100	100	3.00	1.00	100	99	0.00	0.00
	3	7.00	95	0.00	0.00	0.00	0.00	0.00	0.00
	4	8.00	98	0.00	0.00	99	8.00	0.00	0.00
Prediction Damage Case 5 PDE	1	90	91	0.00	0.00	1.00	5.00	0.00	0.00
	2	79	91	7.00	14.00	80	90	6.00	2.00
	3	18.00	90	0.00	0.00	2.00	0.00	0.00	0.00
	4	10.00	90	0.00	0.00	95	12.00	0.00	0.00
	5	13.00	87	1.00	1.00	98	15.00	1.00	0.00
	6	14.00	92	0.00	0.00	1.00	4.00	0.00	0.00

As shown in Table 3, the PoDE is a more accurate damage index, which results in generating smaller errors in both damage cases 4–5. For example, in damage case 4-pattern 4, the braces of Y direction in story 1 are undamaged, however, the PDE value is 8% compared to a 0% PoDE value. The same pattern occurred in damage case 5-pattern 5, where the undamaged braces of Y direction in story 1 show 0% damage, and the probabilistic scheme indicates a 13% probability of damage. It is also indicated that in both cases, the proposed approach provide higher PoDE values compared to the PDE value for the damaged story. The key reason for the higher accuracy of the proposed method in identifying damage elements is the smaller number of surrogate models used in this approach, compared with the probabilistic method presented in previous studies, which in turn results in reducing the prediction error.

Furthermore, as shown in Table 3, all of the actually damaged elements can be successfully identified by the proposed method. Note that  $\theta_{i,y} = \theta_{i,+y} = \theta_{i,-y}$  and  $\theta_{i,x} = \theta_{i,+x} = \theta_{i,-x}$  in this Phase.

Table 4 shows the results of comparing between PoDE, PDE, and direct FE model in terms of computational cost and accuracy. To compute process time when using a surrogate model, data generation time, training and testing time, and WPD implementation time are considered together (core™ i7 2.67 GHz CPU).

It can be concluded from Table 4 that the idea of using a WWLS-SVM model as a surrogate of FE model substantially reduces the computation time of uncertainty based damage detection and maintaining the acceptable detection accuracy. Furthermore, as stated before only two WWLS-SVM models are needed to predict the lower and the lower bounds of ESP. So employing fewer surrogate models in non-probabilistic method reduces the overall prediction error as shown in Table 4.

**Table 4.** Comparison the results in terms of computational cost and accuracy.

Method	RMSE	Total Time (s)
FE model (PDE)	$5.02 \times 10^{-04}$	1202
FE model (PoDE)	$5.02 \times 10^{-04}$	978
Probabilistic WWLS-SVM surrogate model (PDE)	$3.16 \times 10^{-03}$	561
Non-Probabilistic WWLS-SVM surrogate model (PoDE)	$2.01 \times 10^{-03}$	251

### 6.3. Second Phase—Evaluation of Damage Severities

After ensuring the higher ability of PoDE in comparison to PDE, in second phase, the proposed method is trained and examined to predict damage severities of elements. As before, input vectors in Equation (8) are pre-processed from acceleration time histories of the benchmark structure with the assigned severity of damage given by the target values in Table 5.

**Table 5.** Estimates of Damage Severities for Damage Cases 4–5 (DMI).

Damage Case	Damage Patten	Story 1				Story 3			
		$\theta_{i,-y}$	$\theta_{i,+x}$	$\theta_{i,+y}$	$\theta_{i,-x}$	$\theta_{i,-y}$	$\theta_{i,+x}$	$\theta_{i,+y}$	$\theta_{i,-x}$
Target Damage Cases 4&5	1	0.45	0.71	0.45	0.71	0.00	0.00	0.00	0.00
	2	0.45	0.71	0.45	0.71	0.45	0.71	0.45	0.71
	3	0.00	0.36	0.00	0.00	0.00	0.00	0.00	0.00
	4	0.00	0.36	0.00	0.00	0.23	0.00	0.00	0.00
	5	0.00	0.36	0.00	0.00	0.23	0.00	0.00	0.00
	6	0.00	0.23	0.00	0.00	0.00	0.00	0.00	0.00
Prediction Damage Case 4	1	0.44	0.70	0.44	0.70	0.00	0.00	0.00	0.00
	2	0.43	0.70	0.44	0.69	0.44	0.74	0.42	0.68
	3	0.05	0.35	0.01	0.00	0.00	0.00	0.00	0.00
	4	0.00	0.32	0.00	0.01	0.19	0.00	0.02	0.00
Prediction Damage Case 5	1	0.42	0.69	0.40	0.67	0.00	0.00	0.00	0.00
	2	0.40	0.68	0.44	0.70	0.44	0.67	0.40	0.68
	3	0.00	0.30	0.00	0.04	0.00	0.00	0.00	0.00
	4	0.06	0.38	0.00	0.07	0.19	0.01	0.03	0.00
	5	0.00	0.29	0.00	0.00	0.20	0.00	0.04	0.00
	6	0.00	0.18	0.00	0.04	0.00	0.00	0.00	0.00

Maximum damage severity corresponding to structural members in story 2 and 4 (not listed in Table 5) is 0.09.

The results corresponding to the detection of damage severity in the benchmark structural elements in stories 1 to 4 are shown in Table 5. It is noteworthy to indicate that the maximum damage intensity for structural members in the 2nd and 4th floors is 9%, which according to the reference article [50] can be considered healthy, and thus, the damage intensity for these floors is not shown in the Table 5. On the other hand, it is important to state that the effect of loosening the beam on the first floor in the damage pattern 4 and 5 of damage case 5 is negligible [51]. Based on the results shown, it can be concluded that the proposed method accurately determines the severity and the location of damage in the defective members.

### 6.4. Third Phase—Influence of Various Noise Levels on the Identification Results

In the third phase, five sets of WWLS-SVM models are built to study the effect of different noise levels on the identification performance. The models are trained and tested with varying degrees of uncertainty. The rates of uncertainty for the acceleration response are (1) 0%, (2) 2% (SNR = 34 dB), (3) 5% (SNR = 26 dB), (4) 15% (SNR = 16.5 dB), and (5) 20% (SNR = 14 dB). Table 6 shows the PoDE and DMI values for different combinations of uncertainties in the training and testing data. Testing datasets are archived from damage pattern 2-damage case4.

**Table 6.** PoDE and DMI values for damage pattern 2-damage case4.

Train Uncertainties	Element		Test Uncertainties										
			0%		2%		5%		15%		20%		
			PoDE	DMI	PoDE	DMI	PoDE	DMI	PoDE	DMI	PoDE	DMI	
0%	S1	$\theta_{i,y}$	100	0.43	100	0.41	100	0.38	100	0.39	100	0.32	
		$\theta_{i,x}$	100	0.70	100	0.73	99	0.65	85	0.58	85	0.51	
	S2	$\theta_{i,y}$	0	0.00	0	0.00	5.12	0.01	0	0.00	47.1	0.30	
		$\theta_{i,x}$	0	0.00	0	0.00	0	0.00	21.10	0.20	38	0.27	
	S3	$\theta_{i,y}$	100	0.44	99	0.40	100	0.49	80	0.30	95	0.39	
		$\theta_{i,x}$	100	0.71	100	0.69	100	0.65	100	0.79	65	0.40	
	S4	$\theta_{i,y}$	0	0.00	0	0.00	0	0.00	12	0.09	0	0.00	
		$\theta_{i,x}$	0	0.00	0	0.00	0	0.00	0	0.00	13.15	0.09	
	2%	S1	$\theta_{i,y}$	100	0.38	100	0.39	100	0.46	100	0.46	100	0.46
			$\theta_{i,x}$	100	0.68	100	0.67	100	0.69	99	0.69	90	0.69
		S2	$\theta_{i,y}$	0	0.00	0	0.00	0	0.00	19	0.12	39	0.12
			$\theta_{i,x}$	0	0.00	0	0.00	7.12	0.04	17.12	0.10	7.12	0.10
S3		$\theta_{i,y}$	100	0.39	100	0.39	98	0.35	98	0.35	95	0.35	
		$\theta_{i,x}$	100	0.69	100	0.75	100	0.65	94	0.65	90	0.65	
S4		$\theta_{i,y}$	0	0.00	4.11	0.02	0	0.00	0.0	0.00	2.2	0.01	
		$\theta_{i,x}$	0	0.00	0	0.00	0	0.00	4.0	0.04	0	0.00	
5%		S1	$\theta_{i,y}$	100	0.38	100	0.40	100	0.48	100	0.39	79	0.30
			$\theta_{i,x}$	100	0.67	100	0.65	100	0.66	98	0.66	100	0.59
		S2	$\theta_{i,y}$	0	0.00	0	0.00	0	0.00	20.1	0.09	2.1	0.01
			$\theta_{i,x}$	8.16	0.05	6.15	0.04	0	0.04	12.01	0.04	35	0.15
	S3	$\theta_{i,y}$	100	0.46	100	0.39	100	0.41	97	0.49	100	0.41	
		$\theta_{i,x}$	98.11	0.65	100	0.69	100	0.65	100	0.61	76	0.55	
	S4	$\theta_{i,y}$	0	0.00	0	0.00	0	0.00	0	0.00	1.65	0.00	
		$\theta_{i,x}$	0	0.00	0	0.00	0	0.00	10.2	0.12	14.2	0.12	
	15%	S1	$\theta_{i,y}$	100	0.40	100	0.40	100	0.40	100	0.46	78	0.46
			$\theta_{i,x}$	86	0.61	97	0.67	97	0.67	100	0.72	100	0.72
		S2	$\theta_{i,y}$	0	0.00	0	0.00	14.01	0.14	0	0.00	55	0.34
			$\theta_{i,x}$	0	0.00	13.11	0.10	0	0.00	4.41	0.01	0	0.00
S3		$\theta_{i,y}$	100	0.39	100	0.39	100	0.49	100	0.49	87.12	0.37	
		$\theta_{i,x}$	82	0.61	91	0.63	100	0.69	100	0.74	98	0.74	
S4		$\theta_{i,y}$	0	0.00	0	0.00	0	0.00	0	0.00	15.34	0.09	
		$\theta_{i,x}$	0	0.00	0	0.00	0	0.00	0	0.00	0	0.00	
20%		S1	$\theta_{i,y}$	70	0.29	81	0.29	94	0.32	100	0.32	100	0.40
			$\theta_{i,x}$	90	0.60	90	0.60	88.12	0.67	98	0.67	100	0.69
		S2	$\theta_{i,y}$	0	0.00	0	0.00	11	0.03	31	0.13	0	0.00
			$\theta_{i,x}$	54	0.30	33	0.13	0	0.00	14	0.03	0	0.00
	S3	$\theta_{i,y}$	49	0.24	79	0.33	100	0.44	100	0.40	100	0.41	
		$\theta_{i,x}$	61	0.50	80	0.81	100	0.81	100	0.78	100	0.75	
	S4	$\theta_{i,y}$	16.12	0.08	0	0.00	0	0.00	0	0.00	0	0.00	
		$\theta_{i,x}$	38.11	0.17	10.12	0.06	0	0.00	20.1	0.20	0	0.00	

Table 6 shows that at the damaged locations, higher PoDE and DMI values occurred, indicating that the proposed approach can detect damage with noisy data. The table also shows that as the degree of uncertainty increases, the accuracy of the proposed surrogate model decreases. For example, if a WWLS-SVM model trained with 0% uncertainty level in extracted features of acceleration response (deterministic model), the PoDE values will decrease when tested using high-noise data (e.g., 20%). A similar trend can be observed for the DMI index, i.e., it cannot show the exact severity of damage when the relative percentage of noise in the test data increases. The same trend is observed when the model is trained with training data that has a higher noise percentage. For instance, as shown on Table 1, when the WWLS-SVM model is trained with extracted features of the acceleration response, with 20% noise, and tested with 0% noise in the testing data, the accuracy of PoDE and DMI indices decreases.

Based on the various combinations shown in Table 6, it can be concluded that when the noise (i.e., uncertainty) in the training and test data is similar, the highest accuracy is obtained in DMI and PoDE indices. The reliability of the proposed method decreases with increasing the noise percentage difference and ratio between training and testing data. This is due to the fact that when the level of uncertainty in the training and testing data varies from each other, noise contaminates the true information, and thus, the damage cannot be reliably detected. These results indicate the importance of determining the percentage of noise, which is used as a measure of uncertainty, in training data, which in itself requires engineering judgment and prior experience on similar vibration experiments, and therefore,

it can be considered a limitation of the method proposed in this study. However, as shown in Table 3 to Table 6, even when the percentage of noise in the training data is different from the percentage of noise in the test data, the proposed method is more accurate than the probabilistic surrogate method presented in previous studies [12,49].

However, there are still some important details that need to be studied more thoroughly. The best performance of SVM is achieved in supervised mode when training data about health and damage state of structure is available. While in practical cases, it is highly unlikely to have data corresponding to different damage scenarios. Among the four levels of damage assessment identified by Rytter [52], the lowest level (i.e., establishing the presence of damage) has been achieved in the past through unsupervised learning by what is referred to as novelty (outlier) detection [1]. Higher levels of damage assessment in real-world structures require either a mechanism for augmenting the insufficient or incomplete training data by incorporating some form of prior knowledge into the learning and training process [53]. Therefore in real-world application the proposed method can be used as surrogate model of structure in comprehensive SHM system which will be further studied.

## 7. Conclusions

In this research, a non-probabilistic method based on WWLS-SVM algorithm is presented to consider the uncertainties, in the form of noise, in the process of damage detection of structures. An interval analysis is adopted for use with the WWLS-SVM, as an intelligent data analytics scheme, to consider the uncertainties using the interval bounds of the uncertainties in the input parameters of the surrogate model. The proposed framework for damage diagnosis and prognosis is applied to phase I of IASC-ASCE benchmark structure. According to the results summarized in Table 3 to Table 6, it was demonstrated that the health monitoring framework based on WPD, interval analysis and WWLS-SVM has a good capability to detect the presence or absence of damage in the elements, its location and the severity of damage. Therefore, the proposed approach can be used for real time health monitoring of structures with intrinsic uncertainties.

Furthermore, in order to assess the accuracy of the proposed method, influence of different noise levels on the identification results is investigated. The results indicate that the proposed approach is a reliable damage detection technique for a noisy data.

Finally, because of the smaller prediction errors, the proposed non-probabilistic approach can provide more reliable damage detection results than a probabilistic surrogate method. Furthermore, due to the reduced number of surrogate models to be trained, the proposed approach is less time-consuming.

**Author Contributions:** R.G., the first author, was responsible for establishing the methodology introduced in this work and carrying out the majority of the research project. Both analytical derivations and statistical methods were closely tested and confirmed by M.N. and suggested the procedures utilized. W.A.A. provided his expertise and technical background in AI and assisted R.G. with carrying out the numerical analyses and implementation of algorithm. A.S. with his expertise in statistical methods worked closely with R.G. and W.A.A. throughout the project. T.W. worked closely with R.G. in reviewing and editing phase. As a leading scholar and pioneer in SHM and fiber optic sensors, Z.W. offered useful guidance and recommendations that contributed greatly to the conduct of this research project. All authors have read and agreed to the published version of the manuscript.

**Funding:** This research received no external funding.

**Institutional Review Board Statement:** Not applicable.

**Informed Consent Statement:** Not applicable.

**Data Availability Statement:** Publicly available datasets were analyzed in this study. This data can be found here: [https://datacenterhub.org/dataviewer/view/neesdatabases:db/structural\\_control\\_and\\_monitoring\\_benchmark\\_problems/](https://datacenterhub.org/dataviewer/view/neesdatabases:db/structural_control_and_monitoring_benchmark_problems/).

**Conflicts of Interest:** The authors declare no conflict of interest.

## References

1. Avci, O.; Abdeljaber, O.; Kiranyaz, S.; Hussein, M.; Gabbouj, M.; Inman, D.J. A review of vibration-based damage detection in civil structures: From traditional methods to Machine Learning and Deep Learning applications. *Mech. Syst. Signal Process.* **2021**, *147*, 107077. [\[CrossRef\]](#)
2. Farrar, C.R.; Worden, K. *Structural Health Monitoring: A Machine Learning Perspective*; John Wiley & Sons: Hoboken, NJ, USA, 2012; ISBN 1118443217.
3. Toh, G.; Park, J. Review of Vibration-Based Structural Health Monitoring Using Deep Learning. *Appl. Sci.* **2020**, *10*, 1680.
4. Rainieri, C.; Magalhaes, F.; Gargaro, D.; Fabbrocino, G.; Cunha, A. Predicting the variability of natural frequencies and its causes by Second-Order Blind Identification. *Struct. Health Monit.* **2019**, *18*, 486–507.
5. Fathnejat, H.; Ahmadi-nedushan, B. Meta-heuristic algorithms and group method of data handling An efficient two-stage approach for structural damage detection using meta-heuristic algorithms and group method of data handling surrogate model. *Front. Struct. Civ. Eng.* **2020**, *14*, 907–929. [\[CrossRef\]](#)
6. Yang, B.; Lei, Y.; Yang, B.; Jiang, X.; Jia, F.; Li, N.; Nandi, A.K. Applications of machine learning to machine fault diagnosis: A review and roadmap Applications of machine learning to machine fault diagnosis: A review and roadmap. *Mech. Syst. Signal Process.* **2020**, *138*, 106587. [\[CrossRef\]](#)
7. Salehi, H.; Burgueño, R. Emerging artificial intelligence methods in structural engineering. *Eng. Struct.* **2018**, *171*, 170–189. [\[CrossRef\]](#)
8. Azimi, M.; Eslamlou, A.D.; Pekcan, G. Data-Driven Structural Health Monitoring and Damage Detection through Deep Learning: State-of-the-Art Review. *Sensors* **2020**, *20*, 2778.
9. Padil, K.H.; Bakhary, N.; Hao, H. The use of a non-probabilistic artificial neural network to consider uncertainties in vibration-based-damage detection. *Mech. Syst. Signal Process.* **2017**, *83*, 194–209. [\[CrossRef\]](#)
10. Mo, J.; Wang, L.; Qiu, Z.; Shi, Q. A nonprobabilistic structural damage identification approach based on orthogonal polynomial expansion and interval mathematics. *Struct. Control Health Monit.* **2019**, *26*, e2378.
11. Simoen, E.; De Roeck, G.; Lombaert, G. Dealing with uncertainty in model updating for damage assessment: A review. *Mech. Syst. Signal Process.* **2015**, 123–149. [\[CrossRef\]](#)
12. Ghiasi, R.; Ghasemi, M.R. Optimization-based method for structural damage detection with consideration of uncertainties—a comparative study. *Smart Struct. Syst.* **2018**, *22*, 561–574.
13. Bakhary, N.; Hao, H.; Deeks, A.J. Damage detection using artificial neural network with consideration of uncertainties. *Eng. Struct.* **2007**, *29*, 2806–2815. [\[CrossRef\]](#)
14. Shu, J.; Zhang, Z.; Gonzalez, I.; Karoumi, R. The application of a damage detection method using Artificial Neural Network and train-induced vibrations on a simplified railway bridge model. *Eng. Struct.* **2013**, *52*, 408–421. [\[CrossRef\]](#)
15. Qiu, Z.; Wang, L. The need for introduction of non-probabilistic interval conceptions into structural analysis and design. *Sci. China Phys. Mech. Astron.* **2016**, *59*, 114632.
16. Abdulkareem, M.; Bakhary, N. Non-probabilistic wavelet method to consider uncertainties in structural damage detection. *J. Sound Vib.* **2018**, *433*, 77–98. [\[CrossRef\]](#)
17. Ghiasi, R.; Torkezadeh, P.; Noori, M. A machine-learning approach for structural damage detection using least square support vector machine based on a new combinational kernel function. *Struct. Health Monit.* **2016**, *15*, 302–316. [\[CrossRef\]](#)
18. Khatibinia, M.; Gharehbaghi, S. Seismic Reliability-Based Design Optimization of Reinforced Concrete Structures Including Soil-Structure Interaction Effects. In *Earthquake Engineering-From Engineering Seismology to Optimal Seismic Design of Engineering Structures*; Intechopen: London, UK, 2015; pp. 267–304.
19. Suykens, J.A.K.; De Brabanter, J.; Lukas, L.; Vandewalle, J. Weighted least squares support vector machines: Robustness and sparse approximation. *Neurocomputing* **2002**, *48*, 85–105.
20. Padil, K.H.; Bakhary, N.; Abdulkareem, M.; Li, J.; Hao, H. Non-probabilistic method to consider uncertainties in frequency response function for vibration-based damage detection using Artificial Neural Network. *J. Sound Vib.* **2020**, *467*, 115069.
21. Wang, X.; Xia, Y.; Zhou, X.; Yang, C. Structural damage measure index based on non-probabilistic reliability model. *J. Sound Vib.* **2014**, *333*, 1344–1355. [\[CrossRef\]](#)
22. Kankanamge, Y.; Hu, Y.; Shao, X. Application of wavelet transform in structural health monitoring. *Earthq. Eng. Eng. Vib.* **2020**, *19*, 515–532.
23. Ravanfar, S.A.; Razak, H.A.; Ismail, Z.; Hakim, S.J.S. Damage Detection Based on Wavelet Packet Transform and Information Entropy. In *Structural Health Monitoring*; Springer: Cham, Switzerland, 2014; Volume 5, pp. 223–229.
24. Johnson, E.A.; Lam, H.F.; Katafygiotis, L.S.; Beck, J.L. Phase I IASC-ASCE structural health monitoring benchmark problem using simulated data. *J. Eng. Mech.* **2003**, *130*, 3–15.
25. Gurley, K.; Kareem, A. Applications of wavelet transforms in earthquake, wind and ocean engineering. *Eng. Struct.* **1999**, *21*, 149–167.
26. Luckey, D.; Fritz, H.; Legatiuk, D.; Dragos, K.; Smarsly, K. Artificial intelligence techniques for smart city applications. In *International Conference on Computing in Civil and Building Engineering*; Springer: Cham, Switzerland, 2020; pp. 3–15.
27. Yen, G.G.; Lin, K.-C. Wavelet packet feature extraction for vibration monitoring. *IEEE Trans. Ind. Electron.* **2000**, *47*, 650–667.
28. Sun, Z.; Chang, C.-C. Vibration based structural health monitoring: Wavelet packet transform based solution. *Struct. Infrastruct. Eng.* **2007**, *3*, 313–323.

29. Coifman, R.R.; Wickerhauser, M.V. Entropy-based algorithms for best basis selection. *IEEE Trans. Inf. Theory* **1992**, *38*, 713–718.
30. Han, J.-G.; Ren, W.-X.; Sun, Z.-S. Wavelet packet based damage identification of beam structures. *Int. J. Solids Struct.* **2005**, *42*, 6610–6627.
31. Mallat, S.G. A theory for multiresolution signal decomposition: The wavelet representation. *IEEE Trans. Pattern Anal. Mach. Intell.* **1989**, *11*, 674–693.
32. Boller, C. Structural Health Monitoring—An Introduction and Definitions. In *Encyclopedia of Structural Health Monitoring*; Wiley Online Library: Hoboken, NJ, USA, 2009.
33. Daubechies, I. *Ten Lectures on Wavelets*; Siam: Philadelphia, PA, USA, 1992; Volume 61, ISBN 1611970105.
34. Ravanfar, S.A. Vibration-Based Structural Damage Detection and System Identification Using Wavelet Multiresolution Analysis. Ph.D. Thesis, University of Malaya, Kuala Lumpur, Malaysia, 2017.
35. Ghiasi, R.; Torkzadeh, P.; Noori, M. Structural damage detection using artificial neural networks and least square support vector machine with particle swarm harmony search algorithm. *Int. J. Sustain. Mater. Struct. Syst.* **2014**, *4*, 303–320.
36. Nazin, S.A.; Polyak, B.T. Interval parameter estimation under model uncertainty. *Math. Comput. Model. Dyn. Syst.* **2005**, *11*, 225–237.
37. Lantz, B. Black Box Methods—Neural Networks and Support Vector Machines. In *Machine Learning with R*; Jones, J., Sheikh, A., Eds.; Packt Publishing: Birmingham, UK, 2013; pp. 205–242.
38. Rosenblueth, E. Point estimates for probability moments. *Proc. Natl. Acad. Sci. USA* **1975**, *72*, 3812–3814.
39. Cortes, C.; Vapnik, V. Support-vector networks. *Mach. Learn.* **1995**, *20*, 273–297.
40. Suykens, J.A.K.; Vandewalle, J. Least squares support vector machine classifiers. *Neural Process. Lett.* **1999**, *9*, 293–300.
41. Suykens, J.A.K.; Horvath, G.; Basu, S.; Micchelli, C.; Vandewalle, J. *Advances in Learning Theory: Methods, Models and Applications*; IOS Press: Amsterdam, The Netherlands, 2003; ISBN 978-1-58603-341-5.
42. Khatibinia, M.; Javad Fadaee, M.; Salajegheh, J.; Salajegheh, E. Seismic reliability assessment of RC structures including soil–structure interaction using wavelet weighted least squares support vector machine. *Reliab. Eng. Syst. Saf.* **2013**, *110*, 22–33.
43. Seyedpoor, S.M.; Salajegheh, J.; Salajegheh, E.; Gholizadeh, S. Optimum shape design of arch dams for earthquake loading using a fuzzy inference system and wavelet neural networks. *Eng. Optim.* **2009**, *41*, 473–493.
44. He, H.; Yan, W. Structural damage detection with wavelet support vector machine: Introduction and applications. *Struct. Control Heal. Monit.* **2007**, *14*, 162–176.
45. Oh, C.K.; Beck, J.L. A Bayesian learning method for structural damage assessment of phase I IASC-ASCE Benchmark problem. *KSCE J. Civ. Eng.* **2018**, *22*, 987–992.
46. Azimi, M.; Pekcan, G. Structural health monitoring using extremely compressed data through deep learning. *Comput. Civ. Infrastruct. Eng.* **2019**. [CrossRef]
47. Dyke, S. Report on the Building Structural Health Monitoring Problem Phase 1 Analytical. Available online: <https://datacenterhub.org/resources/2806/supportingdocs> (accessed on 1 December 2020).
48. Das, S.; Saha, P. Structural health monitoring techniques implemented on IASC–ASCE benchmark problem: A review. *J. Civ. Struct. Health Monit.* **2018**, *8*, 689–718.
49. Ghasemi, M.R.; Ghiasi, R.; Varae, H. Probability-Based Damage Detection of Structures Using Surrogate Model and Enhanced Ideal Gas Molecular Movement Algorithm. In *Advances in Structural and Multidisciplinary Optimization: Proceedings of the 12th World Congress of Structural and Multidisciplinary Optimization (WCSMO12)*; Schumacher, A., Vietor, T., Fiebig, S., Bletzinger, K.-U., Maute, K., Eds.; Springer International Publishing: Cham, Switzerland, 2018; pp. 1657–1674. ISBN 978-3-319-67988-4.
50. Kook, O.C. *Bayesian Learning for Earthquake Engineering Applications and Structural Health Monitoring*; Earthquake Engineering Research Laboratory: Pasadena, CA, USA, 2007.
51. Yuen, K.-V.; Au, S.K.; Beck, J.L. Two-stage structural health monitoring approach for phase I benchmark studies. *J. Eng. Mech.* **2004**, *130*, 16–33.
52. Rytter, A. Vibrational Based Inspection of Civil Engineering Structures. Ph.D. Thesis, Department of Building Technology and Structural Engineering, Aalborg University, Aalborg, Denmark, 1993.
53. Yuan, F.-G.; Zargar, S.A.; Chen, Q.; Wang, S. Machine learning for structural health monitoring: Challenges and opportunities. In *Sensors and Smart Structures Technologies for Civil, Mechanical, and Aerospace Systems*; SPIE Digital Library; International Society for Optics and Photonics: Bellingham, WA, USA, 2020; Volume 11379, p. 1137903.